AIMS Materials Science, 7(1): 75–92.
DOI: 10.3934/matersci.2020.1.75
Received: 17 December 2019
Accepted: 18 February 2020
Published: 25 February 2020

http://www.aimspress.com/journal/Materials

Research article

Development of tensile fixture with corrugated structure sheet and estimation of tensile strength of glass fibre fabrics based single face corrugated structure sheet

Songtam Laosuwan, Shigeru Nagasawa* and Kazuki Umemoto

Department of mechanical engineering, Nagaoka University of Technology 1603-1 Kamitomioka, Nagaoka, Niigata 940-2188, Japan

*** Correspondence:** Email: snaga@mech.nagaokaut.ac.jp.

Abstract: This work aims to reveal the tensile characteristics of Glass Fibre fabrics based single face corrugated Structure Sheet (GFSS) by developing a pressure-adjustable fixture in the machine producing direction of GFSS. In order to set the fixture quick-ready and stable, the effects of several set-up conditions on the tensile behavior of GFSS were investigated. As the set-up condition, a wavy aluminum block fitted to the surface trace, insertion of multiple flexible pins into wave holes, and double-sided tapes attached on the upper/lower surfaces were discussed by changing the number of pins N, and also a few of instant adhesives was dipped on the clamped/pressured zone of GFSS (the reinforced model). Through this study, the followings were revealed. To use multiple polystyrene pins and several pieces of double-sided tapes in the proposed fixture contributes to make the tensile line force stable (as the simple model: without any instant adhesives on the clamped zone). To perform the breakage of liner and wave layers in the area of the gauge span, the reinforced model is usable when choosing $N > 1$. Investigating the tensile response, the strength (peak maximum line force) and the elongation limit of the liner and wave layers were revealed, respectively. By dipping instant adhesives on the clamping zone when $N > 6$, the combination resistance of liner and wave braiding structure was actualized.

Keywords: tensile strength; flexible pins; wavy fixture; stress concentration; shimming tape

Abbreviations: λ: a wave length (pitch) of GFSS = 7.1 mm; h_o, t_L, t_W: a height of GFSS, a thickness of liner, and a thickness of wave layer; L: the gauge length, 11λ = 78.1 mm (preliminary), 12λ

= 85.2 mm (main); B: a width of specimen, 15 mm; F: a tensile force N, f = F/B: a line force N/mm; d: a displacement of cross head clamping a specimen = an in-plane elongation of the specimen with the gauge span clamped by the fixture; N: numbers of polystyrene pins inserted to wave holes of GFSS specimen; f_{p1}, f_{p2}: the first peak maximum line force and the second peak maximum line force N/mm; $\varepsilon_{p1} = d_{p1}/L$, $\varepsilon_{p2} = d_{p2}/L$: the normalized in-plane elongation of the gauge span area at the first and second peak points, which are corresponding to f_{p1} and f_{p2}; $f_{B(a)}$, $f_{B(b)}$, $f_{B(b')}$ and $f_{B(c)}$: the first maximum line force at the breaking point in the preliminary experiment, (a) a plain sheet of LPC250, (b) a liner layer of GFSS (a wave layer was removed from the clamped zone), (b') a wave layer of GFSS (a liner layer was removed from the clamped zone), and (c) 50 mm length both-end blocks were buried by a solidified unsaturated polyester. See Figure 4, Table 2 and Table 3; κ_1, κ_2: the gradient (tensile stiffness) of line force with the normalized elongation $\kappa_i = \partial f / \partial(d/L)$, i = 1, at increasing zone before the first peak maximum point, i = 2, at increasing zone before the second peak maximum point. Here, the range of 20–80% of the peak maximum line force was chosen for making a linear approximation; $\kappa_{(a)}$, $\kappa_{(b)}$, $\kappa_{(b')}$ and $\kappa_{(c)}$: the gradients of line force with the normalized elongation $\kappa = \partial f / \partial(d/L)$ in the preliminary experiment shown in Figure 4. A linear approximation was applied to the range of 20–80% of the first peak maximum line force.

1. Introduction

Composite materials with glass fibre reinforced polymer are widely used in the automotive industry, transportations and many other industries. Their composite materials have many advantages such as low weight or low density, high stiffness and cheap resources [1–4]. To improve the performance of the glass fibre based composite structure, a geometrical structure of greatly lightweight and a high stiffness are desired. For such requirements, it is possible to use a kind of corrugated fabrics structure. A representative corrugated structure sheet or corrugated fibreboard (CFB), that is widely used for making container boxes, is composed of three layers: the top (outside) liner, the corrugated medium and the back (inside) liner [5–6]. A combination of two layers as a liner and a corrugated medium is called as a single face type. A CFB structure has different properties in the three principal directions [7] as illustrated in Figure 1.

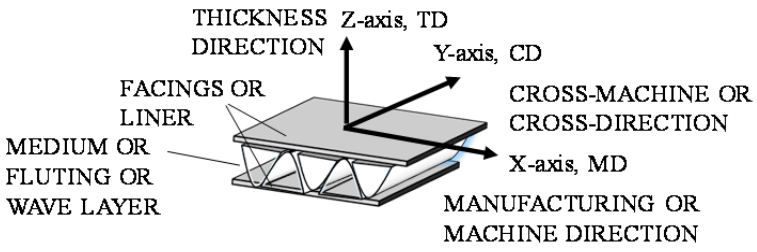

Figure 1. Corrugated fibreboard structure in the three principal directions.

The Glass Fibre fabrics based single face corrugated Structure Sheet (GFSS) seems to be one of suitable choice for using in general purposes [8]. It is composed of the wave and liner layers, which are periodically intersected with each other. The wave layer makes a bridge across the liner layer by knitting as shown in Figure 2.

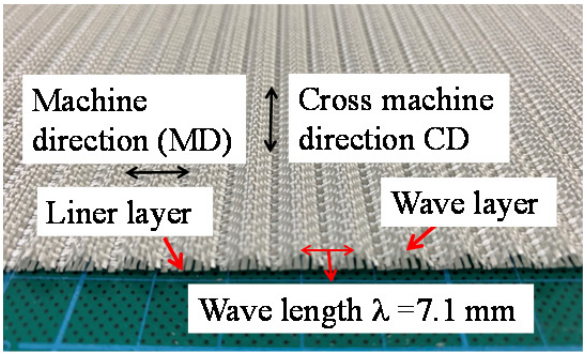

Figure 2. Glass fibre based single face corrugated fabrics sheet.

One of advantages of the GFSS is a good electromagnetic wave transparency, and also the GFSS has the easiness of cylindrical bending and curved wall structure. However, the mechanical properties of the GFSS was not well known in the past due to its complex structure and fragile property. The primary specifications of GFSS are the basic weight or the average density of glass wires, the pitch size of the flute and so on. Regarding the in-plane tensile test of CFB in the producing machine direction (MD), a fixing condition of specimen was explained as a combination of insert pin and wax filling [9]. Wahab et al. [10] studied a fundamental usage of single parallel pin for fixing a double face CFB made of kraft paper. Misra et al. [11] studied the modeling of woven fabric textile composite under in-plain shear loading. Cox [12] has studied effects of orientation of the fibres on the stiffness and strength of paper and other fibrous materials. When seeing the in-plane tensile condition of corrugated paperboards, since the liner and medium layers consisted of wooden strong fibers and they were not fragile against the mechanical fixing by using inner pins and outer fixing plate, the tensile strength of corrugated structure was stably measured and well expected from the raw plain strength of liner or medium parts.

However, since the GFSS was fragile due to its glass fiber based material, appropriate mechanical fixture is necessary for reducing the stress concentration of contact on the fixing device. Nagasawa et al. [13] have studied to estimate the tensile strength of the GFSS by developing a prototype fixture which consisted of parallel pins and thick rubber plate without any wax filling. The mechanical property as the in-plane longitudinal tensile strength are necessary for designing advanced structures, e.g., a packaging box or a shielding wall berried with appropriate solid medium. However, the in-plane tensile strength of the GFSS measured by Nagasawa et al. [13] seemed to be insufficient and largely varied due to the stress concentration and unstable fracture of glass fibres at the clamping zone. Therefore, in this work, to develop an advanced fixture for performing the ultimate strength which was estimated from the plain textile sheet, a corrugated-shaped block was newly introduced and some modifications for reducing the stress concentration on the gripping zone was investigated. That is, a set of flexible parallel pins were inserted to the corrugated medium zone, a bit of instant adhesive was penetrated to the pressure zone of glass fibres, and rapid-acting shimming tapes were attached on the wave and liner layer, in order to perform the reproducibility of the ultimate tensile strength in the longitudinal in-plane direction.

2. Methods of experimental

2.1. Specification of raw materials and profile of tensile test pieces

The raw sheet of GFSS was produced using the twisted yard, E-glass of Nittobo, ECG75-1/2-3.8S (Fineness: 135 (fineness: 135 ± 8.1 TEX, a diameter of filament: 9.5 μm, number of twists: 3.8 per 25 mm) [3,4,8]. Figure 3 is a side view of two waves, which has a wave length (pitch) of λ, a total height h_O, a liner thickness t_L and a wave layer thickness t_W as shown in Table 1.

When the raw sheet of GFSS was knitted, since the flute layer and liner layer were smoothly movable with each other, appropriate gluing was necessary for forming the corrugated-structural profile. After knitting, a few of acrylic based adhesives were injected on the raw sheet of GFSS. The cord count (density) of the upper wave layer and the lower liner of GFSS was 25 ± 1 per 25 mm width in the longitudinal direction (Machine direction) and in the lateral direction (cross machine direction), respectively.

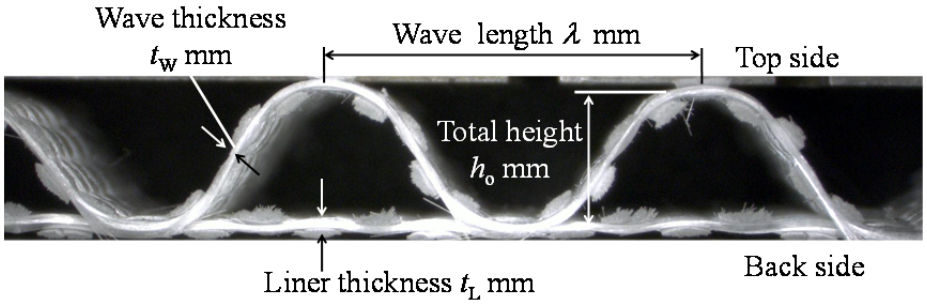

Figure 3. Side view of two flutes of GFSS.

Table 1. Structural dimensions of side view of GFSS.

Geometrical parameters of GFSS shown in Figure 3	Average of 3 samples (maximum-minimum)
Total height, h_o (mm)	2.5 (1.97–2.58)
Wave-length λ (mm)	7.1 (6.86–7.58)
Liner thickness t_L (mm)	0.25 (0.17–0.31)
Wave thickness t_W (mm)	0.25 (0.14–0.30)

2.2. Preliminary estimation of fundamental strength of glass fibre fabrics

In order to reveal the fundamental strength of glass fibre fabrics sheet, each layer (liner and wave layer) should be investigated as a simple structural element, and also an ultimate (uniformly) fixing condition shoud be investigated, before seeing the proposed fixing method of GFSS. Therefore, four kinds of specimen were prepared for knowing the strength of the specimens as the referenced behavior. As the first type specimen, a plain single fabric sheet was prepared for comparing the tensile strength of GFSS. The plain single fabric sheet was a customized sheet LPC250 which consisted of the same glass fibres as that of GFSS. The cord count (density) of LPC250 in the machine direction (MD) was 20 per 25 mm width, and that in the cross machine direction (CD) was 19 per 25 mm width.

Figure 4 shows four kinds of tensile testing specimens (a), (b), (b') and (c) in the Machine direction (transport direction in the manufacturing of fabrics sheet). Here, an extra type of (b') was shown as a side view. Table 2 shows a summary of four kinds of specimens (a), (b), (b') and (c). A width of these specimens was B = 15 mm. The case (a) had an 80 mm gauge length and 56.8 mm clamped both ends which were stacked with the double-sided tape (Nicetack, NW-K15). In the case (b), clamped both ends of liner layer, which have a length of 56.8 mm as 8 waves, were prepared (both ends of wave layer were removed), and stacked with the double-sided tapes. The gauge length was chosen as 78.1 mm which consisted of 11 corrugated waves. Here, as additional case (b'), clamped both ends of wave layer of GFSS (liner layer was removed) were prepared only for discussing the behavior of elongated wave layer. The case (c) had a 78.1 mm gauge span and a pair of 50 mm length blocks which were buried by a solidified unsaturated polyester (UPICA, 4072-PT2). The gauge length of single face corrugated sheet was empirically designed here so as to be close to the standard testing size of kraft liner sheet with JIS P8113. The double-sided tape (NW-15K) was used for joining the holder plates of tensile device and the specimen, and uniformly protecting the fibre fabrics in the cases of (a), (b) and (b'). Here, since the cord count 20 (in MD) of the plain single sheet was different from that (25 in MD) of liner layer and that (25 in MD) of wave layer of GFSS, when comparing the tensile strength as the line force per unit width, an appropriate conversion of line force was necessary. This conversion ratio 25/20 = 1.25 in MD was considered in this work. In order to investigate the fundamental strength of glass fibre fabrics sheet, the prepared four kinds of specimens were pulled by a tensile testing apparatus with the feed velocity of 0.33 mm/s. All the experiments were carried out in the room temperature of 296 K and in the humidity of 50% RH.

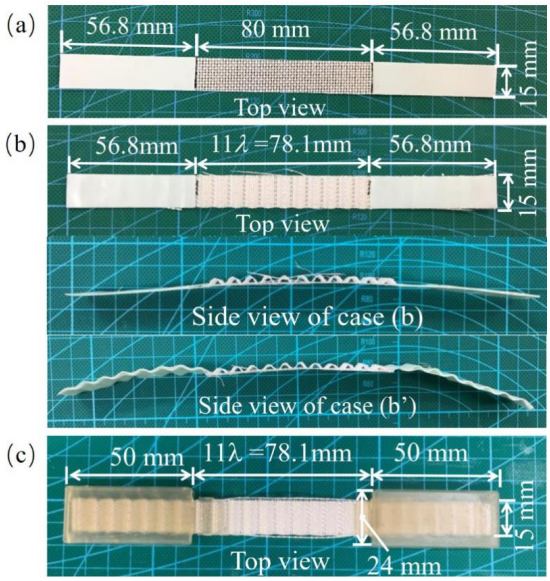

Figure 4. Four kinds of mechanical conditions (plain sheet, liner layer, wave layer and gripped by solidified block) for preliminary tensile testing in Machine direction. (a) Specimen of plain single layer sheet stacked with double-sided shimming tapes, (b) Specimen of liner layer of GFSS stacked with double-sided shimming tapes (wave layer of clamped zone was removed). Specimen of wave layer of GFSS (liner layer of clamped zone was removed) was considered as (b'), (c) Specimen of GFSS gripped by 5 mm thickness resin solidified block (unsaturated polyester).

Table 2. Summary of four kinds of preliminary tensile testing without multiple pins.

Type of mechanical condition of specimen and fixture	Span length, cord count in MD	Purpose of investigation
(a) Plain sheet LPC250	80 mm, 20	To know the strength of simple plain sheet
(b) Liner sheet of GFSS (wave layer was removed)	78.1 mm, 25	To know the strength of liner layer of GFSS in MD
(b') Wave sheet of GFSS (liner layer was removed)	78.1 mm, 25	To know the strength of wave layer of GFSS in MD
(c) Solidified resin block with GFSS	78.1 mm, 25	To know the strength of GFSS in MD

2.3. Setup of fixture on GFSS specimen in MD

In the report of Nagasawa et al. [13], the gauge length was assumed to be 13 waves of 7.1 mm pitch and this span was a little long/inconvenient for measuring in the tensile test apparatus. In this work, the gauge length L was modified as 85.2 mm = 12 waves of 7.1 mm pitch. Regarding the clamping zone, in order to investigate the effect of the number of inserted pins N on the tensile deformation of GFSS, the inserted pins were considered from single pin to seven pins (N = 1, 2, 3, 4, 5, 6 and 7 for each side of the gripper). Figure 5 shows a layout of GFSS specimen, which includes 7 polystyrene pins at the left zone and 7 polystyrene pins at the right zone. On the upper/lower outsides of specimen, double-sided tapes NW-K15 were pasted at the clamping zone. This taping was considered in order to make the contact pressure reduced at the clamping zone. The Young's modulus and the hardness number of the polystyrene bar/pin (soft type) were about 756 MPa and 8.6 VHN, respectively. When replacing the polystyrene pins to steel parallel pins, the tensile strength of GFSS was empirically reduced. Hence, the polystyrene pins were used in this work.

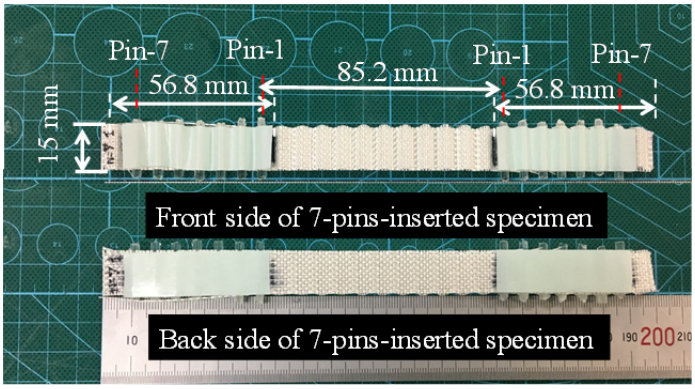

Figure 5. A prepared GFSS specimen for tensile testing in MD. The gauge length of 85.2 mm was estimated as 12 waves of 7.1 mm pitch, and the left (or right) side gripping length was 56.8 mm = 8 waves of 7.1 mm was prepared. NW-K15 double sided tapes were pasted on the outside of liner and wave layer, while seven flexible parallel pins of 3 mm diameter were inserted to the wave holes. The numbers of parallel pins N were varied from 1 up to 7, as the inside pins were left for gripping and the outside pins were removed, respectively.

For fixing the specimen at the clamping zone, the previous study [13] used a urethane rubber fixture with 2.5 mm thickness and 70(A) shore hardness. However, this gripping seemed to be insufficient for uniformly reducing the contact pressure at the clamping zone of 7-waves. Therefore, a new curve-fitted solid fixture, named as the wave block, (made of aluminum alloy A5052) was developed as shown in Figure 6.

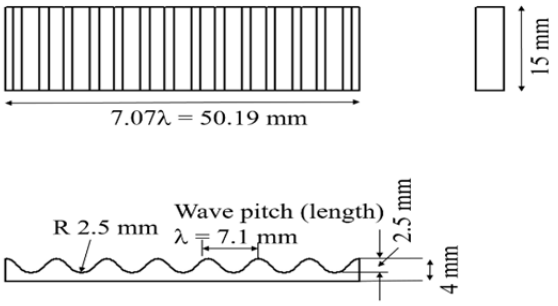

Figure 6. Sketched drawing of a wave block for clamping the wave layer.

Figure 7 shows an example of left side fixture composed of a wave block, double-sided tapes, four 3 mm diameter polystyrene pins and claw blocks of tensile testing apparatus. The right side fixture is similarly set up with the same specimen of GFSS. The number of 3-mm-diameter pins were chosen as N = 1, 2, 3, 4, 5, 6 and 7 on the left side fixture. That of the right side fixture were considered as the symmetric condition. The closest pins between the left side and right side had the gauge length L of 12 waves × 7.1 mm pitch = 85.2 mm. After setting the fixture up on a specimen of GFSS, the tensile testing was carried out, under a feed velocity of 0.33 mm/s, a sampling rate of 30 points/s.

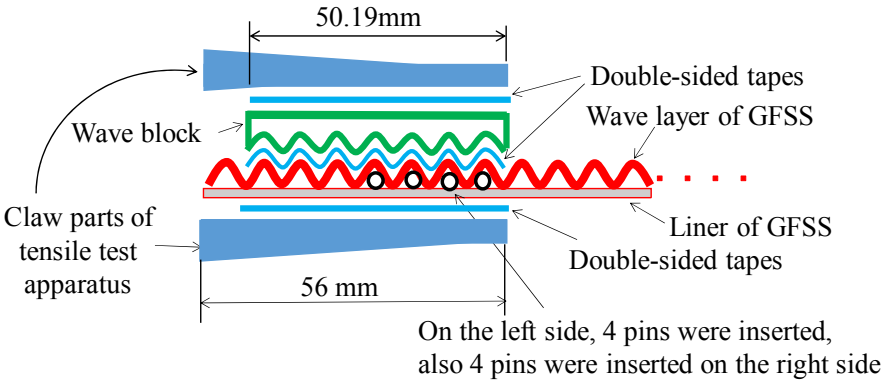

Figure 7. Configuration of fixture on the left side using a wave block, double-sided tapes, flexible pins (illustrated in case of four pins on the left side) and claw parts of tensile testing apparatus.

In order to reveal the effect of resin reinforcement, as shown in Figure 8, a brief-reinforcement of clamping zone was considered by dipping a few of instant adhesives to the clamping zone against the flexible pins. Although the case (c) is an ultimate gripping condition, to fully solidify the clamping

zone takes a long time and additional preparation. Therefore, as a brief-reinforced condition, to drop 4.4 g of liquid instant adhesives to the clamping zone for each inserted pin (e.g., cyanoacrylate based adhesives, such as Arone alpha, Krazy glue) was examined and discussed about its effect.

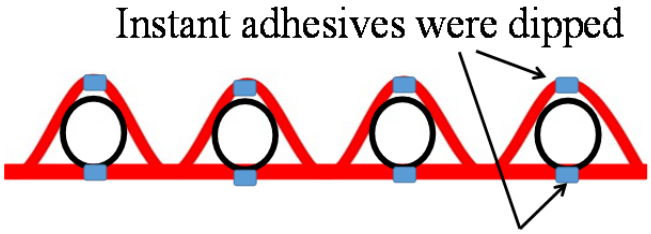

Figure 8. A brief-reinforced condition of clamping zone at one side when using eight pins for clamping. One time drop of 0.73 g (= 4.4 g/6 points) instant adhesives (liquid arone alpha) was dipped to the surface of upper wave layer and the lower liner layer at 3 positions (left/middle/right) on a width of 15 mm.

2.4. Experimental condition

When varying the number of flexible pins N = 1, 2, 3, 4, 5, 6 and 7, the GFSS specimen clamped by the fixture was elongated by a tensile apparatus with a velocity of 0.33 mm/s until reaching the breakage of wave layer in a temperature of 296 K and a relative humidity of 50% RH. Five pieces of GFSS specimen were examined for the preliminary, and eight pieces were examined for the basic and reinforced models. During this tensile test, the relationship between the tensile line force $F/B = f$ (the force per unit width of the specimen) and the normalized elongation d/L (= the non-dimensional claw displacement) against the gauge length L was recorded. Also, the video image by a VHX digital microscope was recorded for knowing the breakage behavior of clamping zone and contact-free zone.

3. Results and discussions

3.1. Fundamental strength of glass fibre fabrics

Four kinds of mechanical conditions were considered for investigating the fundamental in-plane tensile strength of glass fibre fabrics in Machine direction, as shown in Figure 4 and Table 2: (a) plain sheet, (b) liner layer, (b') wave layer and (c) GFSS using solidified resin block. Figure 9 shows representative tensile line force responses of four kinds of mechanical conditions with respect to the normalized elongation of gauge length L when the in-plane tensile testing was applied to the specified sheet with a feed velocity of 0.33 mm/s. Table 3 shows the breaking strength as the maximum line force and the normalized breaking elongation with the four kinds of mechanical conditions. Here, the final breakage of specimens was observed in a range of gauge span.

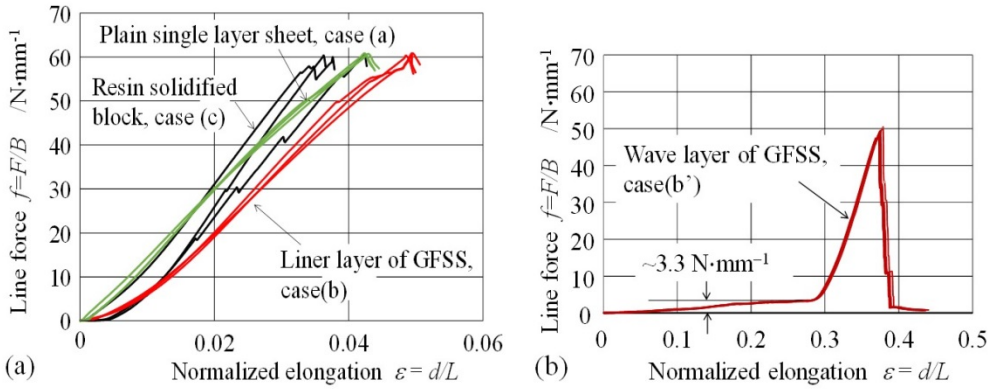

Figure 9. Tensile line force response of four kinds of sheets shown in Figure 4 with respect to the normalized elongation. Here, the number of samples were three for each case.

Table 3. In-plane tensile strength of four kinds of glass fibre fabrics sheets. Average of 5 samples (standard deviation).

Type of mechanical condition of fixture	Breaking (maximum) line force f_B (N/mm)	Normalized breaking elongation ε_B against the gauge length L
(a) Plain sheet LPC250, L = 80 mm	60.6 (0.26), as converted using the cord count ratio 25/20	0.041 (0.003)
(b) Liner sheet of GFSS (wave layer was removed), L = 78.1 mm	60.7 (0.32)	0.049 (0.005)
(b') Wave sheet of GFSS (liner layer was removed), L = 78.1 mm	47.1 (0.94)	0.367 (0.006) Difference: 0.087 = 0.367–0.28 (0.006)
(c) Solidified resin block with GFSS, L = 78.1 mm	60.3 (0.31)	0.039 (0.003) at the first peak point

Seeing the results of cases (a), (b), (c) in Table 3, it was revealed that the liner layer of GFSS had the tensile strength of about 60 N/mm when the cord count was 25, and the tensile strength of GFSS was primarily determined from that of the liner layer. It was found that the tensile strength of the wave layer of GFSS (case (b')) was less than that of liner layer (case (b)), although the wave layer had the same cord count as the liner layer. From this result, it seemed that the fibres of wave layer were damaged by a wavy forming when knitting the wave layer to the liner layer. Namely, the wave layer appeared to have a certain residual stress from the wavy forming. In the case (b'), a difference of breaking elongation 0.087 was calculated as a difference between a displacement of fixture 0.367 and a starting position of load increasing (~3.3 N/mm) in the straight-tensile state 0.28. As for the tensile behavior of GFSS in the case (c), there were two peak maximum line forces. The behavior of secondary peak is discussed in the later when seeing the results of tensile test of GFSS using the multiple pins and wave block. Only the first peak line force and its breaking normalized elongation were picked up. Comparing the strength of plain sheet LPC250 (case (a)) with that of liner layer of GFSS (case (b)), it was confirmed that the tensile strength of MD sheet could be stably evaluated as considering the equivalent cord count. According to the previous report by Nagasawa et al. [13], the first breaking strength of line force of GFSS was about 30 N/mm when

using a rubber fixture plate and 6 pins (= 3 pins x the left and right sides). It was found that this value of 30 N/mm was almost a half of the current result shown in Table 3 (cases (a), (b) and (c)).

The in-plane tensile gradient (stiffness) of $\kappa = \partial f / \partial(d/L)$ was linearly approximated from the load responses in Figure 9. Here, the range of 20–80% of the breaking strength (line force) was chosen for fitting a linear relation. The averaged gradients with the three kinds of mechanical conditions were $\kappa_{(a)}$ = 1584 N/mm, $\kappa_{(b)}$ = 1544 N/mm, and $\kappa_{(c)}$ = 1967 N/mm, respectively. As for the wave layer tensile condition, the average gradient was $\kappa_{(b')}$ = 601 N/mm. Assuming that the apparent thickness of plain sheet was t_L=0.25 (from Table 1), in-plane apparent tensile moduli were estimated as $E_{(a)} = \kappa_{(a)}/t_L$= 6.3 GPa, $E_{(b)} = \kappa_{(b)}/t_L$ = 6.2 GPa, respectively. According to the public opened data of mechanical properties of E-glass from Nittobo [14], since the E-glass filament had a Young's modulus of E = 75 GPa, apparent tensile moduli of the specified sheets of the cases (a), (b) were about 10% of the filament stiffness. In the case (c), although the wave layer was slidable against the liner layer due to its braiding, since a loosen but soft triangle structure was constructed between the liner and wave layer under a frictional constraint, the stiffness $\kappa_{(c)}$ was 27% larger than $\kappa_{(b)}$. In the case of wave layer tensile, it was found that the maximum line force was 77.6% (= $f_{B(b')}/f_{B(b)}$ = (47.1/60.7) × 100) of the liner layer, and also the gradient (tensile stiffness) was 38.9% (= $\kappa_{(b')}/\kappa_{(b)}$ = (601/1544) × 100) of the liner layer.

3.2. Representative tensile behavior of GFSS using multiple pins and wave block

Figure 10 shows the relationship between the tensile line force f N/mm and the normalized elongation d/L against a gauge length of L = 85.2 mm, while Figure 11 shows side views of GFSS specimen at some positions: d/L = 0.0 (starting), 0.04 (the first peak P_1), 0.09 (an intermediate between the first and second peak) and 0.37 (the second peak P_2).

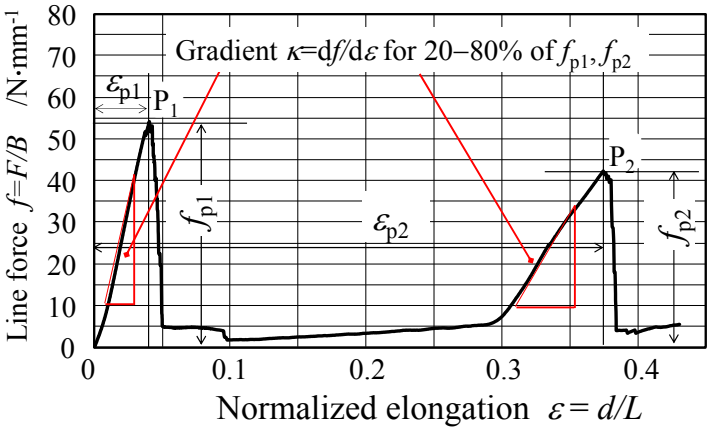

Figure 10. An example of tensile line load response of GFSS specimen shown in Figure 5 and Figure 7 with respect to normalized elongation d/L. Here, a gauge length L was 85.2 mm, a number of inserted pins was N = 7, a width of specimen was B = 15 mm and a feed velocity was 0.33 mm/s.

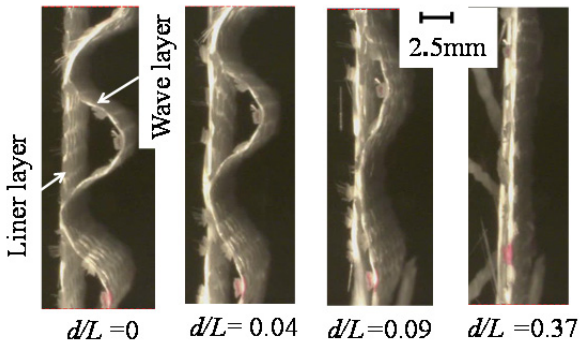

Figure 11. Side views of GFSS specimen during a tensile testing, when watching several positions: d/L = 0.0 (the starting position), 0.04 (the first peak position), 0.09 (an intermediate position between the first peak and the second peak points) and 0.37 (the second peak position). Here. A gauge length was L = 85.2 mm.

Seeing Figure 10 at the first peak P_1 (d/L = 0.04) and Figure 11 (at d/L = 0.09), the wave layer was extended without breaking but the liner layer was broken at clamping zone. Namely, the load peak P_1 was related to a breaking state of the liner layer at the clamping zone. Figure 12 shows representative top views of a liner layer at d/L = 0.04 (before the peak point P_1) and a wave layer at d/L = 0.47 (after the second peak P_2) when setting N = 7. Near the first peak maximum line force, the glass fibres of the liner layer were broken on one side (there are the left and right sides of clamping) in the tensile direction. Here, searching the breaking pattern with 8 samples at the first peak position, the initial breakage was detected at the clamping zone (as shown in Figure 12a) with 62% occurrence while it was detected at the gauge span area with 38% occurrence. When reaching d/L = 0.37, the second load peak occurred and the wave layer was broken in a range of the gauge span as shown in Figure 12b. Through this tensile testing, it was found that the liner layer was firstly stretched and make the first peak load f_{p1}, while the wave layer was firstly loosened and secondly stretched after a certain delay.

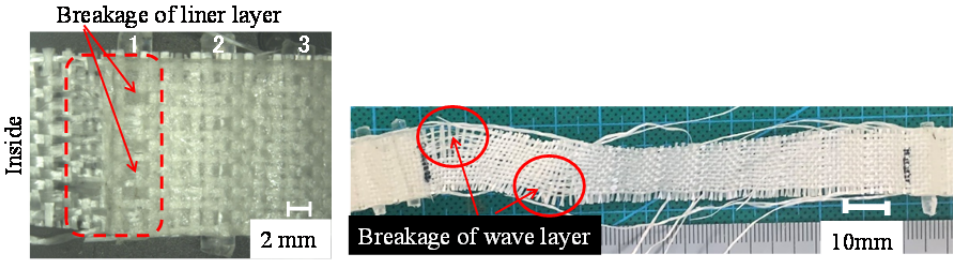

(a) Liner layer at d/L=0.04 (before first peak maximum)

(b) Wave layer at d/L=0.47 (after second peak maximum)

Figure 12. A representative top view (out-of-plane) of (a) a liner layer around No.1 pin clamped at the first peak point P_1, and (b) a wave layer after the second peak point P_2, using the simple model in case of N = 7. Some glass-fibre cords of liner layer were split in the lateral direction (tensile direction) around the No.1 clamped position of inserted pins in (a), while that of wave layer were split in a range of the gauge span (free from constraint of fixture) in (b).

Seeing a duration from d/L = 0.04 to 0.09 in Figure 10, the line force had a kind of residual resistance 5 N/mm and decreased to 2 N/mm. It was seemed that the breakage of the liner layer had not completely performed and finished at d/L = 0.09–0.1 mm. The second increasing of line force started at d/L = 0.28 (d = 23.8 mm) and reached the peak f_{p2}, which was related to the breaking strength of the case (b'). Since this distance from the first increasing point (d = 0 mm) seemed to be determined from the length difference of wave layer against the liner layer, the arc length difference of the wave layer was estimated using the approximation of Eq 1 for describing a cycle of the wave layer of GFSS. Putting $s(x)$ as the arc length of the wave layer, $(\mathrm{d}s/\mathrm{d}x)^2$ as Eq 2 was derived from Eq 1.

$$y(x) = (h/2)(1 + \sin(2\pi x/\lambda)) \quad \text{for a range from } x = -\lambda/4 \text{ up to } x = 3\lambda/4 \tag{1}$$

$$(\mathrm{d}s/\mathrm{d}x)^2 = (\mathrm{d}y/\mathrm{d}x)^2 + 1 = (\pi h/\lambda)^2\cos^2(2\pi x/\lambda) + 1 \tag{2}$$

Numerically integrating the derivative function $\mathrm{d}s/\mathrm{d}x$ with x from $x = -\lambda/4$ up to $x = 3\lambda/4$, the wave length of one cycle was 8.93 mm, when h = 2.5 mm, λ = 7.1 mm and the integration range was divided with 40 increment. As the arc difference of s-λ was 1.83 mm for one cycle, the total arc length of 12 waves was estimated as d = 22 mm (d/L = 0.26). This value was fairly close to the measured span length of d/L = 0.28. So far, the secondary increasing of line force and its peak occurrence were understood as the elastic extension of the wave layer and its final breaking. In Figure 10 from d/L = 0.1 up to 0.28, there is a small gradient of $\kappa \approx 8$ N/mm (1.3% of $\kappa_{(b')}$). This small increasing response is corresponded to a sort of expanding deformation of curled wave layer fabrics. Namely, since the wave layer was curled and twisted state, compared to the liner layer, the tensile strength and the gradient (tensile stiffness) seemed to be weakened (reduced) and softened in a little extent.

The first peak f_{p1}, shown in Figure 9, was about 92% of 60 N/mm (case (b) shown in Table 3), and the second peak f_{p2} was about 96% of 47 N/mm (case (b') shown in Table 3) when N = 7 in the simple model.

3.3. Peak maximum line force and elongation with respect to the number of inserted pins

When the number of inserted pins was chosen as N = 1, 2, 3, 4, 5, 6 and 7, the In-plane tensile test of GFSS specimen shown in Figure 5 and 7 was carried out. The peak maximum line forces f_{p1}, f_{p2} and corresponded normalized elongation ε_{p1}, ε_{p2} were arranged from the load response. Also, the gradient of $\partial f/\partial(d/L) = \kappa$ was analyzed at the increasing stages: 20–80% of f_{p1}, f_{p2}.

Figure 13 shows f_{p1}, f_{p2}, ε_{p1} and ε_{p2} as the average and the standard deviation of measured samples when choosing the number of inserted pins N=1, 2, 3, 4, 5, 6 and 7. Here, parts of the fixture were stacked and assembled by double-sided tapes as shown in Figure 7 without any instant adhesives (the basic model).

In Figure 13, although the pin number was a natural number, assuming that it was a real number, the increment rate of $\partial f_{p1}/\partial N$ was equivalently calculated as around 3.3 N/mm when varying N from 1 up to 7. The peak maximum line force was affected by the number of inserted pins. f_{p1} tended to be larger than f_{p2} for $N > 3$, while $f_{p1} \approx f_{p2}$ (around 40 N/mm) for $N < 3$. Seeing the numbers of inserted pins, $N > 7$ seems to be better for performing the strength of $f_{p1} > 60$ N/mm, while the strength of f_{p2} was settled down in 90–98% of 47 N/mm (Table 2 (b')). As for the

elongation of peak position, $\varepsilon_{p1} \approx 0.05$, $\varepsilon_{p2} \approx 0.37$ (i.e., the breaking elastic elongation: 0.09 = 0.37–0.28) for $N = 1, 2, 3, 4, 5, 6$ and 7. The corresponded elongation (the first breaking point with the liner layer, and the second breaking point with the wave layer) were almost independent from the number of inserted pins. In order to investigate the effects of resin painting on the tensile strength of clamped zone, the clamped zone of GFSS were reinforced by dipping instant adhesives (i.e., Arone alpha was examined) as shown in Figure 8 (a reinforced model).

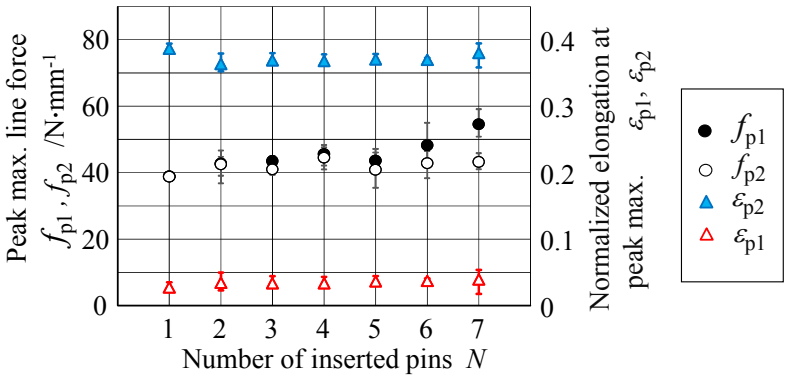

Figure 13. The first and second peak maximum line forces f_{p1}, f_{p2} and corresponded normalized elongation ε_{p1}, ε_{p2} when choosing the number of inserted pins N = 1–7 at a simple stacking condition. The fixture was composed of wave block and multiple 3 mm polystyrene pins as shown in Figure 7. Parts of the fixture were stacked and assembled using double-sided tapes, here the clamping zones were simply stacked without any instant adhesives (the simple model). Average of six samples (error bars were based on the standard deviation) was plotted.

Figure 14 shows f_{p1}, f_{p2}, ε_{p1} and ε_{p2} as the average and the standard deviation of measured samples when choosing the number of inserted pins $N = 1, 2, 3, 4, 5, 6$ and 7 in the case of reinforced model.

Since f_{p1}, f_{p2} with the basic model shown in Figure 13 were 92–96 % of the strength of the preliminary experiment (Table 3 (b) and (b')), the liner and wave layer seemed to be slightly damaged by the use of the fixture (Figure 7), and the initial breaking seemed to occur at the clamping zone. Using the reinforced model, f_{p1} increased with the number of inserted pins N as shown in Figure 14, and the incremental rate of $\partial f_{p1}/\partial N$ was around 3.0 N/mm. This incremental rate was almost equal to that of the simple model. In the current work of reinforced model, the largest f_{p1} was around 80 N/mm at N = 7, due to a limitation of the testing machine and equipment adopted. An upper bound strength 107.8 N/mm, a sum of $f_{B(b)}$ = 60.7 and $f_{B(b')}$ = 47.1 N/mm, is expected from Table 3, if the ultimate breaking strains of wave and liner layer were synchronized. But the strain of wave layer and that of liner layer do not match with each other, against the common elongation d/L. The most isolated state is recognized as the case (b) in Table 3. When using the reinforced model by dipping instant adhesives on the clamping zone, since the fixture restrains the clamping zone of the wave and liner layers in a certain extent, the ultimate breaking force f_{p1} is affected by the deformation of wave layer, as well as determined by that of liner layer. This relationship is expressed as Eq 3. Here, a coefficient $\alpha = 0.41$ was estimated when $N = 7$ in the reinforced model.

$$f_{B(b)} < f_{p1} < f_{B(b)} + \alpha \cdot f_{B(b')} \qquad (0<\alpha<1) \qquad (3)$$

f_{p1} was larger than $f_{B(b)}$ = 60 N/mm for N >1. Hence, the reinforced model supplies a stable condition to make the liner layer of GFSS in an ultimate tensile state when using multiple pins. Searching the breaking pattern in the reinforced model, the initial breakage occurred in the gauge span area when changing N from 1 to 7. Comparing the value of f_{p1} = 80 N/mm at the reinforced model (N = 7) with the preliminary result $f_{B(c)}$ = 60 N/mm in the case (c), although they should be almost same with each other, the latter was not increased state. This seems to be caused from the mechanical differences: the solidified block resin was not so hard; the wave holes were not filled with flexible pins, and then a certain resistance of rotation, shear resistance by clamping would be insufficient.

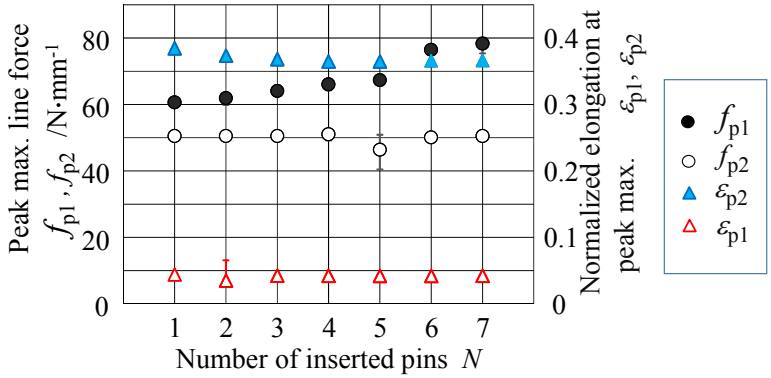

Figure 14 The first and second peak maximum line forces f_{p1}, f_{p2} and corresponded normalized elongation ε_{p1}, ε_{p2} when choosing the number of inserted pins N = 1–7 and dipping instant adhesives on the clamping zone (the reinforced model). The fixture condition was same as the basic model condition, except for dipping instant adhesives on the clamping zone. Average of six samples (error bars were based on the standard deviation) was plotted.

On the contrary, f_{p2} was about 50 N/mm, almost equal to $f_{B(b')}$. The corresponded elongation ε_{p1}, ε_{p2} were almost equal to that of the basic model. Therefore, it was found that the dipping of instant adhesives onto the liner and wave layers of GFSS reinforced the clamped zone with the first peak maximum load. Figure 15 shows representative top views of a liner layer at the first peak point P_1 and a wave layer after passing the second peak point P_2 in a case of the reinforced model when N = 7. The breakage mainly occurred in the area of the gauge span as shown in Figure 15a, although a bit of small breakage was sometimes observed near the No.1 pin's clamping zone. Since the breakage of wave layer after passing P_2 occurred in the area of the gauge span as shown in Figure 15b, it was revealed that the value of f_{p2} was characterized/determined by the strength of glass fibre cords with the wave layer, but not by the number of inserted pins.

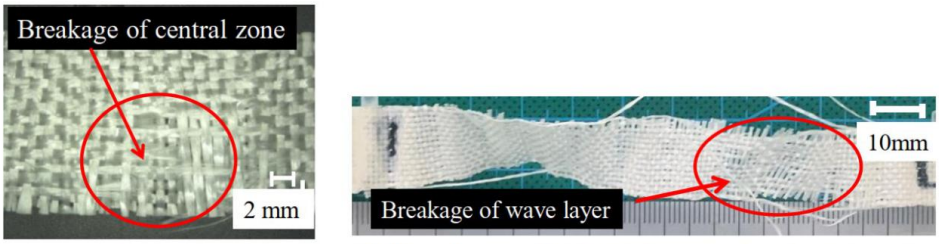

(a) Liner layer at d/L=0.04 (before first peak maximum)

(b) Wave layer at d/L=0.47 (after second peak maximum)

Figure 15. A representative top view (out-of-plane) of (a) a central area of the liner layer at the first peak point P_1, and (b) a wave layer after the second peak point P_2, using the reinforced model in case of N = 7. A few of glass-fibre cords of liner layer were split in the lateral direction (tensile direction) at a central area in case of (a), while that of wave layer were split in a range of the gauge span (free from constraint of fixture) in case of (b).

3.4. Tensile stiffness of liner and wave layers at load increasing process

Figure 16 shows gradients (tensile stiffness) of load increasing against the elongation $\kappa_i = \partial f / \partial(d/L)$, i = 1: before the first peak and i = 2: before the second peak with two clamping conditions (simple and reinforced models) when changing N = 1, 2, 3, 4, 5, 6 and 7. To dip Arone alpha liquid on the clamping zone makes the gradient larger than the gradient of the simple model. The following features were revealed: (1) The first gradient κ_1 was stably about 1500 N/mm ($\approx \kappa_{(b)}$) with the simple model, while its increasing rate with the numbers of inserted pins was around 9 times in the case of reinforced model. (2) The κ_1 was affected (increased) by the numbers of inserted pins N. It reached around 2000 N/mm at N = 6. The weaving triangle structure of wave and liner seemed to be constrained by the distributed gluing on the clamping zone. Since the case (c), which used block fixtures buried by a solidified unsaturated polyester, had a gradient of $\kappa_{(c)}$ =1967 N/mm, the reinforced model (for N = 6, 7) was appeared to reach a level of full solidified state. (3) The second gradient κ_2 of the simple model and that of the reinforced model were about 520 (86.5% of $\kappa_{(b')}$), 730 (121.5% of $\kappa_{(b')}$) N/mm, respectively. As the κ_2 was mainly determined by stretching of the gauge span area of wave layer, it was basically independent to a variation of the number of inserted pins N.

Synthetically, it was revealed that the reinforced model enabled to make the first peak breakage of liner layer in the gauge span area, also the second peak breakage of wave layer occurred in the gauge span area when N > 1. As for the tensile stiffness (load gradient against elongation) κ_1, the simple model is useful for estimating the stiffness of liner layer. When choosing N > 6 with the reinforced model, both the first peak force f_{p1} and the tensile stiffness κ_1 are appeared to be affected by the geometrical constraint of wave and liner weaving structure.

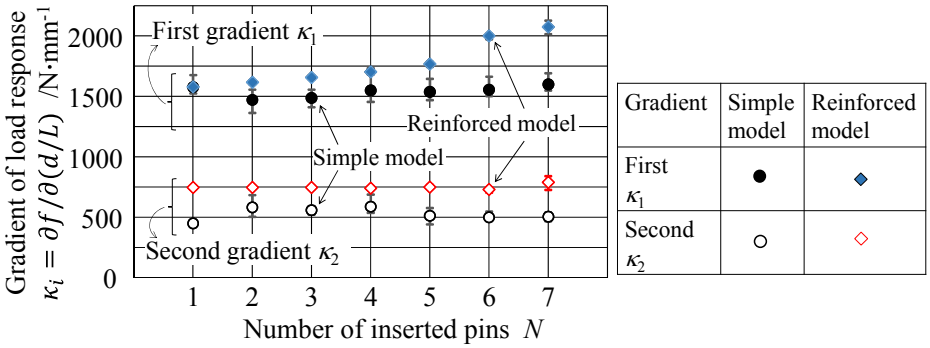

Figure 16. Comparison of gradient of load increasing against elongation $\kappa_i = \partial f/\partial(d/L)$, i = 1: before the first peak and i =2: before the second peak with two clamping conditions (simple and reinforced models) when changing the number of inserted pins.

4. Conclusions

In order to perform an in-plane tensile testing of fragile glass fibre based single faced corrugated structure sheet (GFSS), and to reveal its fundamental strength and elongation limit, a compact fixture composed of flexible inserted pins, light wave block, double-sided shimming tapes and additional dip of instant adhesives for reinforcing clamped/contact zone was developed. To discuss the in-plane tensile strength and stiffness of GFSS, several preliminary experiments were investigated (four kinds of conditions: a plain sheet, wave and liner layers were inspected individually, and fully solidified wave and liner layers was also inspected). The revealed results were as follows:

1. A prototype specimen which has a width of 15mm, a gauge length of 11 waves (L = 7.1 × 12 = 85.2 mm) and a pair of clamping zone of 8 waves (1–7 waves were used for inserting flexible pins) was successfully examined. In the tensile testing, there are two peak maximum line forces (tensile strength): the first peak line force f_{p1}, the second peak line force f_{p2}, and their corresponding elongations against the gauge length $\varepsilon_{p1} = d_{p1}/L$, $\varepsilon_{p2} = d_{p2}/L$ were detected.
2. The first and second peak points were related to the liner and wave layer breakages respectively, in the basic model (without dipping any instant adhesives on the clamped zone). The interval displacement of these two peak points matched the difference of wave length against the liner length. Its theoretical estimation was d/L = 0.26, while the experimentally measured result was d/L = 0.28.
3. The basic model, when choosing the number of inserted pins N = 7, is fairly close to the preliminary experimental level, but the tensile strength (f_{p1}) was insufficient yet for N < 6, due to a damage of clamping condition. From the preliminary experiment, the tensile strength of the liner layer as $f_{B(b)}$ was about 60 N/mm, and that of wave layer $f_{B(b')}$ was about 47 N/mm. Although the glass fibre cord of liner and wave layers was the same specification, the strength of wave layer was weaker than that of liner layer through the tensile analysis, due to the difference of forming process.
4. The normalized elongations at the peak points 1, 2 were $\varepsilon_{p1} \approx 0.05$, $\varepsilon_{p2} \approx 0.37$ when choosing N = 1, 2, 3, 4, 5, 6 and 7 with both the basic and reinforced models. Comparing with

preliminary experiment, $\varepsilon_{p1} \approx \varepsilon_{B(b)} = 0.049$ and $\varepsilon_{p2} \approx \varepsilon_{B(b')} = 0.367$, respectively. Namely, the two kinds of breaking limit of elongations, which are related to the liner and wave layers, are stably measured using the proposed fixture method.

5. The first peak line force f_{p1} increases with N from 1 up to 7. The variation rate was $\partial f_{p1} / \partial N \approx$ 3.0–3.3 N/mm for the basic and reinforced models, assuming that N behaves a real number. The second peak line force f_{p2} was independent to N due to breaking patterns in the gauge span area. Its value was about 0.9 $f_{B(b')}$ with the basic model and 1.06 $f_{B(b')}$ with the reinforced model, respectively.
6. The first gradient (tensile stiffness) of basic model κ_1 was about $\kappa_{(b)}$ for N = 1, 2, 3, 4, 5, 6 and 7, and the κ_1 of reinforced model was about $\kappa_{(b)}$ at N = 1 but larger than $\kappa_{(c)}$ = 1967 N/mm for $N > 6$.
7. To perform the breakage of liner and wave layers in the area of the gauge span, the proposed reinforced model based on dipping of instant adhesives on clamping zone is usable when choosing $N > 1$.
8. To use multiple polystyrene pins and several pieces of double-sided tapes in the proposed fixture device contributes to make the tensile line force response stable (as the simple model). However, since the level of f_{p1} is insufficient in the simple model when $N < 7$, to dip instant adhesives on the clamping zone is necessary for performing a relation of $f_{p1} > f_{B(b)}$ when $N > 1$.
9. Eq 3 describes the behavior of the in-plane strength of GFSS when the fixture constrains the clamped zone.

Acknowledgements

The authors thank Syotaro Takeda of KUBO corporation, for his assistance with preliminary experiments and preparing glass fibre based fabrics structural sheets.

Conflict of interests

All authors declare no conflicts of interest in this paper.

References

1. Caproni G, Tagliferri V (1995) Damage development in drilling glass fibre reinforced plastics. *Int J Mach Tool Manu Int* 35: 817–829.
2. Mehbudi P, Baghlani V, Akbari J, et al. (2013) Applying ultrasonic vibration to decrease drilling-induced delamination in GFRP laminates. *Procedia CIRP* 6: 577–582.
3. Loewenstein KL (1973) *The Manufacturing Technology of Continuous Glass Fibres*, 1st Ed., New York: Elsevier, 2–94.
4. Loewenstein KL (1975) The manufacture of continuous glass fibres. *Platin Met Rev* 19: 84–87.
5. Van Nostrand Reinhold (1982) Characterization of corrugated board, In: Lubin G, *Handbook of Composite*, 1st Ed., Boston: Springer, 145–149.
6. Steadman R (2002) Characterization of corrugated board, In: Mark RE, Borch J, Habeger C, *Handbook of Physical Testing of Paper*, 2 Eds., New York: CRC Press, 1: 571–574.

7. Dekker A (2013) Corrugated fiberboard packaging, In: Kirwan MJ, *Handbook of Paper and Paperboard Packaging Technology*, 2 Eds., New Jersey: Wiley-Blackwell, 313–321.
8. Jonson G (1999) *Corrugated Board Packaging*, 2 Eds., Leatherhead: Pira International, 145–159.
9. Kubo Corporation, Glass fibre based structural sheet. 2017. Available from: http://www.kubo-co.net/.
10. Matsushima S, Okuda T, Miyauchi O, et al. (1982) Strength of tensile deformation for corrugated fibre board. *Jpn Tappi J* 36: 377–387.
11. Wahab N, Arafah A, Fukuzawa Y, et al. (2016) Estimation of corrugated cardboard strength using tensile test. *Proceedings of Mechanical Engineering Research Day*, 1–2.
12. Cox HL (1952) The elasticity and strength of paper and other fibrous materials. *Br J Appl* 3: 72–79.
13. Nagasawa S, Kudo H, Songtam L, et al. (2017) Tensile characteristics of glass fibre based single face board. *Procedia Eng* 207: 78–83.
14. Niitobo Corporation, Mechanical properties of E-glass. 2019. Available from: https://www.nittobo.co.jp/business/glassfiber/about/composition.htm.

AIMS Press